Williamsburg, Virginia
ACTIVE 04
2004 September 20-22

Generation of Higher Order Modes in a Rectangular Duct

Carl H. Gerhold
NASA
Langley Research Center
MS 461
Hampton, VA, 23681
carl.h.gerhold@nasa.gov

Randolph H. Cabell
NASA
Langley Research Center
MS 463
Hampton, VA, 23681
randolph.h.cabell@nasa.gov

Donald E. Brown
Jacobs Sverdrup
NASA-LaRC
MS 901
Hampton, VA, 23681
d.e.brown@larc.nasa.gov

ABSTRACT

Advanced noise control methodologies to reduce sound emission from aircraft engines take advantage of the modal structure of the noise in the duct. This noise is caused by the interaction of rotor wakes with downstream obstructions such as exit guide vanes. Mode synthesis has been accomplished in circular ducts and current active noise control work has made use of this capability to cancel fan noise. The goal of the current effort is to examine the fundamental process of higher order mode propagation through an acoustically treated, curved duct. The duct cross-section is rectangular to permit greater flexibility in representation of a range of duct curvatures. The work presented is the development of a feedforward control system to generate a user-specified modal pattern in the duct. The multiple-error, filtered-x LMS algorithm is used to determine the magnitude and phase of signal input to the loudspeakers to produce a desired modal pattern at a set of error microphones. Implementation issues, including loudspeaker placement and error microphone placement, are discussed. Preliminary results from a 9-3/8" by 21" duct, using 12 loudspeakers and 24 microphones, are presented. These results demonstrate the ability of the control system to generate a user-specified mode while suppressing undesired modes.

1. INTRODUCTION

The high bypass-ratio aircraft engine, such as the powerplant for the Boeing 777, utilizes a turbojet core to drive a large ducted fan. The engine's thrust is predominantly from the fan. Such a high bypass ratio engine, in addition to being more fuel efficient than a pure jet, greatly reduces jet noise as an environmental pollutant. The fan is a major noise source, which includes broadband noise and coherent noise in tones at the blade passage frequency and at its harmonics. The most common way of reducing this noise is through the use of acoustic lining that is applied to the interior surfaces of the bypass duct. A cut away drawing of the ducted fan engine is shown in figure 1. The bypass duct downstream of the fan may curve as shown in order to accommodate various design constraints. This curve in the aft bypass duct, by breaking the line of sight, could enhance the efficiency of the acoustic liner. A curved duct project has been started at NASA to quantify the effect of curvature on noise reduction in a lined duct. The control system that is the subject of this paper is an integral part of the curved duct project.

Optimal noise control in ducts requires knowledge of the physical characteristics of the sound that propagates in the duct. One way to characterize the sound in a duct is by the propagating modes (1). This modal description is particularly useful in the case of coherent sound, such as that produced by the interaction of the rotor wakes with downstream obstructions in the fan bypass duct (2). When the mode structure is known in the duct, the sound that is propagated to the far field can be estimated (3,4,5). Knowledge of the mode structure in a circular duct was used in an active control system on a 0.305 m diameter test ducted fan (6). Rotor/stator interaction produced a known modal structure in the duct in a tone at the blade passage frequency. A circumferential array of loudspeakers generated control sound in the duct in a modal pattern that mimicked the noise source. The pattern was rotated by adjusting the phase of the signals to the loudspeakers until the sound power at an array of wall-mounted reference microphones was

minimized. The control system demonstrated that reducing the fan noise in the duct reduces the noise that is radiated into the acoustic far field. The success of this control system relied on an assumed modal structure in the duct, which could be hard-wired into the control loudspeaker array. Other active noise control experiments programs have investigated the use the modal structure of the sound in the duct to enhance controllability (7) or to assess the sensitivity of control to the distribution of control sources (8,9). The presence of air flow in the duct is a significant parameter in the selection and distribution of sound sources in ducts where control of the structure of sound is a goal of the experiment (10). Most of these studies are limited to plane waves in the duct or to mode structures that are defined a priori by the control source configuration. In a previous experiment, a control system was developed for the purpose of generating arbitrary combinations of acoustic sound patterns at a specified frequency in a 0.305 m diameter duct (11). Specified duct modes were obtained in the duct by controlling the amplitudes and phases to a circumferential array of wall-mounted loudspeakers. The control sources were distributed circumferentially on a circular duct at one axial station. This arrangement permits high controllability of the circumferential modes but compromises controllability of the radial modes.

In the current project, an adaptive feedforward control system is used to drive a single mode in a rectangular duct at a specified frequency, to the exclusion of other modes which are cut on at that frequency. Twelve loudspeakers and 24 microphones, mounted on the walls of a 0.533 m x 0.233 m test duct, are used as actuators and sensors. The feedforward control system uses the multiple-error filtered-X LMS algorithm (12,13,14). The control system will eventually be used in a metal duct with flow, however the duct described in this paper has been configured specifically for control system development. It is a hardwall rectangular duct with anechoic terminations at either end.

2. CONTROL SYSTEM

The duct mode control system is a real-time, multi-input, multi-output (MIMO) controller capable of handling 24 microphones and 12 speakers. The control system has been designed to generate 3D acoustic pressure profiles corresponding to the (m,n) acoustic pressure mode in a rectangular duct.

A. Basis functions

The control system is based on the solution for acoustic wave propagation p(x,y,z,t) in a hard-walled rectangular duct of cross section height a and width b. The sound pressure for a harmonic wave of frequency, ω can be expressed as:

$$p(x,y,z,t) = e^{i\omega t} \sum_m \sum_n (A_{mn}^{+} e^{-ik_z z} + A_{mn}^{-} e^{ik_z z}) \cos(\tfrac{m\pi x}{a}) \cos(\tfrac{n\pi y}{b}) \quad (1)$$

where:

m = mode number in the x-direction (integer)

n = mode number in the y-direction (integer)

A_{mn}^{+} = Amplitude of the (m, n) mode wave traveling in the positive axial direction

A_{mn}^{-} = Amplitude of the (m, n) mode wave traveling in the negative axial direction

k_z = Axial wavenumber of the (m, n) mode,= $\sqrt{k^2 - (\tfrac{m\pi}{a})^2 - (\tfrac{n\pi}{b})^2}$

$k = \omega / c$

c = Speed of sound in air

The desired modal response at each microphone for a single user-defined mode can be computed using Equation 1. The error between the desired microphone response and the measured microphone response is used in the control system to determine the amplitude and phase of signal that is supplied to each input channel. The controller uses the time domain filtered-x LMS algorithm to drive the multiple speakers outputs to produce the correct amplitude and phase at each microphone.

B. Control Algorithm

The block diagram of the control system is shown in figure 2. In a typical feedforward control system, a reference signal that is highly coherent with the disturbance noise is sampled and used by the controller. However, in the current application, the goal is not to cancel noise from a disturbance, but to produce a specified pattern of amplitudes and phases at the error microphones at a desired frequency. This means the reference signal at the frequency of interest can be generated by the control system itself. In this manner, the coherence between the reference signal and the error microphone responses at the frequency of interest is maximized.

A two-coefficient, finite impulse response filter is used to control the amplitude and phase of the tone supplied to each loudspeaker. A two-coefficient filter is sufficient to produce an arbitrary amplitude and phase shift of an input sinusoid. A tapped delay line of the reference signal is often used for implementing an adaptive finite impulse response filter. However, to improve convergence speed, in-phase and quadrature (90 degree phase-lag) versions of the reference signal are generated. One coefficient of the filter multiplied the in-phase signal, and the other multiplied the quadrature signal. In this manner, the coefficients are orthogonal, thereby improving the convergence speed of the adaptive algorithm. The error at each microphone is calculated in real-time as the difference between the desired modal response and the measured microphone signal. The multiple error filtered-x LMS algorithm is used to update the value of the two coefficients for each channel based on the error values calculated for each microphone. When the error is minimized, convergence is achieved. The error (in dB) is defined as:

$$error = 10\log_{10}\left(\frac{\sum_{i=1}^{N_{mic}}(measured - desired)^2}{\sum_{i=1}^{N_{mic}}(desired)^2}\right) \quad (2)$$

Identification of the transfer functions between each speaker and microphone pair at the operational frequency is done before the controller is started each day. This allows for easy compensation of day-to-day changes in system parameters and configurations. These estimated transfer functions ensure correct phasing of the coefficient update in the adaptive algorithm.

C. Hardware and Software Environment

The hardware for the control system consists of a host PC and a control computer running a real-time embedded operating system. The embedded operating system allows for rapid execution of the feedback control algorithm at sampling rates up to 5 kHz. The control computer interfaces to the wall-mounted microphone and speaker signals through A/D and D/A boards.

The controller software was developed using Mathworks Simulink and Real-Time workshop on the Host PC. The control system was first modeled and tested using Simulink on the Host PC. The model was then compiled and downloaded to the control computer using the Mathworks Real-Time Workshop with the xPC target compiler.

3. ANALYSIS OF SOUND PRESSURE DATA IN THE DUCT

This section describes how the acoustic pressure in the duct is used to characterize the sound field by defining the amplitude and phase of the propagating modes.

A finite number of modal terms, corresponding to the cut-on modes in the duct, are chosen and Equation 1 is expanded neglecting the common frequency term:

$$
\begin{aligned}
p(x,y,z) &= (A_{00}^{+}e^{-ik_{00}z} + A_{00}^{-}e^{ik_{00}z}) + (A_{01}^{+}e^{-ik_{01}z} + A_{01}^{-}e^{ik_{01}z})\cos\left(\frac{\pi y}{b}\right) + \ldots + \\
&+ (A_{0N}^{+}e^{-ik_{0N}z} + A_{0N}^{-}e^{ik_{0N}z})\cos\left(\frac{N\pi y}{b}\right) + (A_{10}^{+}e^{-ik_{10}z} + A_{10}^{-}e^{ik_{10}z})\cos\left(\frac{\pi x}{a}\right) + \\
&+ (A_{11}^{+}e^{-ik_{11}z} + A_{11}^{-}e^{ik_{11}z})\cos\left(\frac{\pi x}{a}\right)\cos\left(\frac{\pi y}{b}\right) + \ldots + \\
&+ (A_{1N}^{+}e^{-ik_{1N}z} + A_{1N}^{-}e^{ik_{1N}z})\cos\left(\frac{\pi x}{a}\right)\cos\left(\frac{N\pi y}{b}\right) + \ldots + \\
&+ (A_{M0}^{+}e^{-ik_{M0}z} + A_{M0}^{-}e^{ik_{M0}z})\cos\left(\frac{M\pi x}{a}\right) \\
&+ (A_{M1}^{+}e^{-ik_{M1}z} + A_{M1}^{-}e^{ik_{M1}z})\cos\left(M\frac{\pi x}{a}\right)\cos\left(\frac{\pi y}{b}\right) + \ldots + \\
&(A_{MN}^{+}e^{-ik_{MN}z} + A_{MN}^{-}e^{ik_{MN}z})\cos\left(\frac{M\pi x}{a}\right)\cos\left(\frac{N\pi y}{b}\right)
\end{aligned}
\tag{3}
$$

The sound pressure is sampled at N_{mic} locations across the duct. The resulting steady state pressure is cast into the form of a linear equation:

$$
\{p\} = [\ \mathrm{T}\ ]\{A\}
$$

$$
= \begin{bmatrix}
e^{-ik_{00}z_1}\ldots e^{-ik_{MN}z_1}\cos\left(\frac{M\pi x_1}{a}\right)\cos\left(\frac{N\pi y_1}{b}\right) & e^{ik_{00}z_1}\ldots e^{ik_{MN}z_1}\cos\left(\frac{M\pi x_1}{a}\right)\cos\left(\frac{N\pi y_1}{b}\right) \\
e^{-ik_{00}z_2}\ldots e^{-ik_{MN}z_2}\cos\left(\frac{M\pi x_2}{a}\right)\cos\left(\frac{N\pi y_2}{b}\right) & e^{ik_{00}z_2}\ldots e^{ik_{MN}z_2}\cos\left(\frac{M\pi x_2}{a}\right)\cos\left(\frac{N\pi y_2}{b}\right) \\
\ldots & \\
e^{-ik_{00}z_{N_{mic}}}\ldots e^{-ik_{MN}z_{N_{mic}}}\cos\left(\frac{M\pi x_{N_{mic}}}{a}\right)\cos\left(\frac{N\pi y_{N_{mic}}}{b}\right) & \ldots e^{ik_{MN}z_{N_{mic}}}\cos\left(\frac{M\pi x_{N_{mic}}}{a}\right)\cos\left(\frac{N\pi y_{N_{mic}}}{b}\right)
\end{bmatrix}
\begin{Bmatrix}
A_{00}^{+} \\ \ldots \\ A_{MN}^{+} \\ A_{00}^{-} \\ \ldots \\ A_{MN}^{-}
\end{Bmatrix}
\tag{4}
$$

The vector {p} is of length N_{mic} and the complex pressure amplitudes are all known from measurement. The transfer matrix [T] has N_{mic} rows and 2MN columns and each row of the matrix [T] contains the terms of equation (3). All the coefficients of the transfer matrix are known from the measurement locations (x,y,z) defined for each microphone. The unknown coefficients which define the modal amplitudes of each forward and backward traveling wave are in the solution vector {A} which is of length 2MN. The solution vector is obtained by solving the set of linear equations shown in equation (4). A Singular Value Decomposition method may be preferred if the transfer matrix is poorly conditioned.

A. Determining Modes In The Duct.

The axial wavenumber in the duct without flow was defined in equation 1 as:

$$
k_z = \sqrt{k^2 - (\tfrac{m\pi}{a})^2 - (\tfrac{n\pi}{b})^2}
$$

where:

$$
k = \omega / c
$$

In order for sound to propagate in the duct, it is necessary for k_z to be real. The frequency at which $k_z = 0$ is the cut-on frequency of the (m,n) mode. Table I summarizes the values of cut-on frequency for the present duct. Since all cut-on modes in the duct must be controlled, and each cut-on mode has a forward- and a backward-traveling component, an error-sensing array of 24 microphones is valid, theoretically, as long as no more than 12 forward and 12 backward propagating modes are cut on in the duct.

4. EXPERIMENT SET-UP

The duct mode experiment uses an existing reinforced plywood duct that was used in previous duct noise investigations. It has been modified for this experiment.

A. Test duct

Figure 3 shows a diagram of the duct. The coordinate system that defines the duct is x- horizontal, y- vertical, and z- axial. The duct is approximately 6.10 m long, and has a sidewall dimension of 0.233 m wide by 0.53 m high. It is closed at both ends using a hard wall and modified foam wedges (0.914 m long) as anechoic terminations. There are two major components to the duct instrumentation: the sound source and the wall-mounted array of microphones.

B. Sound Source

User-defined sound is generated using 12 JBL loudspeakers (Model 2485J), oriented in two axial locations of six loudspeakers as shown in Figure 3. The loudspeakers on either side of the duct are directly across the duct from one another. They penetrate the duct wall at three locations on the long wall, at 5%, 50%, and 95% of the wall height. Sound is directed into the duct using a transition piece from 50.8 mm round to a 25.4 mm by 88.9 mm rectangular slot. The long side of the slot is oriented along the axis of the duct so that the source appears, as much as possible, to be a point source along the vertical dimension. The loudspeakers are driven by 12 Carver amplifiers (Model TFM-42). The input to the amplifiers is from the D/A converters, which is the control system output.

C. Wall-mounted array

The wall-mounted array consists of 24 Kulite microphones (Model XCQ-093) randomly distributed on the top and right sides of the duct. Table II lists the location of each wall-mounted microphone with respect to the first microphone.

The reference location of the wall-mounted array is approximately 2.15 m. from the front edge of the first axial plane of the loudspeakers. A NEFF 495 Dynamic data acquisition system is used to provide signal conditioning consisting of excitation and amplification for each channel. The signals from each microphone channel are conditioned with Precision Filter anti-aliasing filters set to a low-pass cut-off frequency of 2kHz.

The control computer acquires data from the wall-mounted array by three UEI 8 channel 16-bit A/D input boards. The data analysis and control processes are discussed in a later section of this report.

D. Offline Data Acquisition and Analysis

Once the control system has reached steady state (indicating that the control system has converged on the selected mode), a block of data are sampled from the 24-microphone wall-mounted array. The signal to one of the loudspeakers is also sampled as a reference.

Data from the 24 microphone channels of the sidewall array are acquired by a NEFF 495 high speed data acquisition system at a sample rate of 20,000 samples/second in records of 4 seconds duration.

The voltage data are converted into sound pressure using the complex-valued conversion factors measured for each microphone during calibration. The time data are segmented into a series of non-overlapping blocks containing 2048 samples each and Fast Fourier Transforms (FFT) are performed using a Hanning window. The reference frequency bin is selected from the reference signal, and the vector of complex acoustic pressure {p} for the microphones is formed. The number of cut-on modes is evaluated for the selected frequency and the transfer function matrix [T] is evaluated. The set of linear equations is solved using Singular Value Decomposition, from which the modal amplitude vector {A} (reconstructed pressure field) is determined.

E. Calibration

The complex-valued term defining the overall sensitivity of the complete instrumentation stream (including the microphone, signal conditioner, and data acquisition) is determined using a B&K model 4260 multi-

frequency calibrator. The microphone sensor channel response is recorded at excitation frequencies of 125, 250, 500, 1000, and 2000 Hz. The signal exciting the driver in the calibrator is recorded simultaneously so that magnitude and phase of the sensor channel response can be evaluated.

5. RESULTS

The purpose of the control system is to generate a user-specified mode in the duct. The criterion for success is that the modal decomposition of the sound pressure in the duct shows that a) the specified mode is present in the duct, and b) its amplitude is much greater than any other mode in the duct.

Tests were performed to quantify the mode generation capability of the control system. The control system was operated at frequencies up to 1610 Hz, which is slightly above the frequency of the highest mode that can be resolved by the sidewall array. A desired mode is generated at a frequency and the resultant steady state sound pressures at the sidewall array are recorded and analyzed. The modes and frequencies were chosen to test the system for two cases. In the first case, the frequency at which a mode is generated is far removed from any cut-on frequency. Up to 3 tests are performed at each frequency at different mode values. The frequencies and modes are identified in Table III. In the second case, the frequency is just above the cut-on frequency of a mode. The barely cut-on mode is generated in one test, and in a second test a mode of lower order is generated. The purpose of this second case is to evaluate whether the controller can generate lower order modes in the presence of a near cut-on mode. The frequencies and modes for the second case are identified in Table IV.

An example of the modal decomposition results using the sidewall array is shown in figure 4. In this first case example, the frequency is set at 970 Hz, and the specified mode is the (1,1). Note that 970 Hz is approximately 0.4% above the cut-on of the (0,3) mode. The figure shows that the (1,1) mode is dominant in the duct and that the incident wave is approximately 10 dB greater than the reflected. Other modes are present in the duct, but they are at least 13 dB less than the dominant mode.

A figure of merit that is checked for each of the decompositions is to synthesize the sound pressure at each microphone based on the calculated modal amplitudes. This synthesized sound pressure distribution is compared to the original measured sound pressure at each microphone. One such comparison of results at 1150 Hz for the selected mode (1,1) is shown in figure 5. The synthesized sound level is comparable to the measured sound level. The peaks and valleys are in the same locations for the synthesized and measured sound levels.

Table III summarizes the results of the case in which the excitation frequency is not near any mode cut-on frequency. One mode is selected for generation (up to three selections at each frequency) and is identified in the table in columns headed “Selected mode 1”, “Selected mode 2”, and “Selected mode 3”, respectively. Table IV summarizes the results of the case in which the system is operated at frequencies near cut-on of the mode that is identified in the “Mode nearest cut on” column. The cut-on ratio, which is the ratio of the excitation frequency to the frequency at which the mode cuts on, is identified in each instance. Generally, the frequency selected is within 1% of mode cut-on. One mode is selected for generation (two selections at each frequency) and is identified in the table in columns headed “Selected mode 1” or “Selected mode 2”. One of the modes selected is the mode nearest cut-on and one is of a lower order. Each selected mode in Tables III and IV is accompanied by a column labeled “Mode Amplitude Ratio”. The parameter is the difference, in dB, between the incident wave modal amplitude of the selected mode and the amplitude of the next highest mode and thus is an evaluation of the controllability. A positive value for the mode amplitude ratio indicates that the incident (forward-traveling) component of the selected mode has the largest amplitude.

When the excitation frequency is not near a cut-on, the system is generally able to control the desired mode at frequencies up to 1550 Hz, as is seen from Table III. The selected mode is dominant in the duct, as indicated by positive values of the mode amplitude ratio in all but 2 cases at frequencies below 1550 Hz, and the dominant mode is at least 8.5 dB greater than the next mode in all but 2 cases. The controller was not able to generate the desired mode at all above 1550 Hz.

The results in Table IV indicate that, for the most part, the selected mode dominates when it is generated near its cut-on frequency. The notation R on three of the mode values indicates that the wave is in a resonance condition. The wave has, essentially, zero propagation speed. The incident and reflected components of the mode are equal, and it is not possible to control their relative amplitudes. The NC (no convergence) next to the (2,2) mode at 1610 Hz indicates that the controller did not converge on this selected mode. When the desired mode was just barely cut on as shown in the column "Selected mode 2", it was dominant for modes up to 2 on the short side of the duct or 4 on the long side. When the desired mode was below the cut-on as shown in the column "Selected mode 1", it had the highest amplitude about as often as not.

6. DISCUSSION OF RESULTS

The control system is able to generate the desired mode for most set points of the tests of both cases. Of 41 combinations of mode number and frequency, the specified mode is greatest in all but 12 as indicated by a positive value for the mode amplitude ratio.

The 12 modes that the control system fails to generate acceptably are of particular interest. They are listed in Table V and discussed in the following paragraphs.

The system is not capable of controlling the 4^{th} order modes on the long side of the duct, such as (0,4), or 2^{nd} order modes on the short side, such as (2,0), with reliability. In fact, in one case, the controller could not even converge. The reason these modes cannot be controlled is thought to be due to the fact that loudspeaker distribution lacks the spatial resolution to generate these higher order modes.

There are 5 cases where a lower order mode failed to dominate when the frequency was just above cut-on of higher order. Three of these instances are attributable to the lack of spatial resolution in the sound sources. It is not immediately clear why the system converged on the wrong mode in the two remaining cases and converged on the desired mode in other cases. When the desired mode was driven at a frequency near its cut-on, the mode was dominant, within the limits of the spatial resolution of the sound sources; but in three instances a resonance condition was generated so that the incident and reflected waves could not be controlled separately. One of the purposes of this test was to determine whether the system could control modes at near cut-on conditions and it was found that, while the desired mode was generated, control of the incident and reflected components is not reliable.

The system is found to capable of generating the desired mode when the frequency is not purposefully chosen to be near a mode cut-on, within the limits of the spatial resolution of the sound sources.

7. CONCLUSIONS

A control system has been successfully implemented which generates higher order modes in a rectangular duct without flow. The control system has been shown to converge to the desired mode for a majority of cases in the duct. In a few cases, the control system indicates that it has converged, but the standing wave nearer to a cut-on frequency actually dominates. It is found that the control is not reliable when the driving frequency is within approximately 1% of a mode cut-on frequency, no matter what mode is specified. The system was tested over a range of frequencies and modes including those high enough that the system fails to converge. The relationship between the distribution of drivers and mode order that can be generated has been determined.

ACKNOWLEDGEMENTS

The authors wish to acknowledge the contributions of Beverly Anderson, NASA, Brian Howerton, Lockheed Martin, and Phil Grauberger, Analytical Services and Materials for their aid in fabrication of the test facility, set up of the instrumentation, and collection of the acoustic data.

8. REFERENCES:

1. Tyler, J.M. and Sofrin, T.G., "Axial Flow Compressor Noise", SAE Transactions, vol 70, pp 309-322, 1962

2. Sutliff, D, Konno, K, and Heidelberg, L, “Duct Mode Measurements on the TFE 732-60 Full Scale Engine”, AIAA-2002-2564, 2002
3. Rice, E.J. and Heidman, .M.F., “Modal Propagation Angles in a Cylindrical Duct with Flow and Their Relationship to Sound Radiation”, AIAA-79-0183, 1979
4. Thomas, R.H., Farassat, F., Clark, L.R., Gerhold, C.H., Kelly, J.J., and Becker, L.E., “A Mode Detection Method Using the Azimuthal Directivity of a Turbofan Model”, presented at the 5th AIAA/CEAS Aeroacoustics Conference, May, 1999
5. Gerhold, C.H.,” Determination of Fan Inlet Duct Mode Structure Using In-duct Microphone Array Measurement, presented at 141st Meeting of the Acoustical Society of America, June , 2001
6. Gerhold, C.H., "Active Control of Fan-Generated Tone Noise", AIAA Journal, vol. 35, no. 1, pp 16-22, January, 1997
7. Smith, J.P., Burdisso, R.A., Sutliff, D.L., and Heidelberg, L.J., “Active Control on a Large-Scale Ducted Fan Inlet with Wavenumber Sensing”, presented at 139th meeting of the Acoustical Society of America, May, 2000.
8. Mangiante, G, “Source Distributions for Active Control of Sound in Ducts of Finite Length”, proceedings of Active 2002, pp 233-242, INCE, July, 2002.
9. Walker, B, “Sensitivity Issues in Active Control of Circular Modes Using Axially-Spaced Actuator Arrays”, proceedings of Active 99, pp 99-105, INCE, December, 1999
10. Johnson, M.E. and Fuller, C.R., “Development and Testing of a High Level Axial Array Duct Sound Source for the NASA Flow Impedance Test Facility”, NASA/CR-2000-210645, December, 2000.
11. Silcox, R.J. and Lester, H.C., “Sound Propagating Through a Variable Area Duct: Experiment and Theory”, AIAA-81-1967, 1981
12. Morgan, D.R. (1980) "An Analysis Of Multiple Correlation Cancellation Loops With A Filter In The Auxiliary Path." IEEE Transactions on Acoustics, Speech, and Signal Processing. ASSP-28, 454-467.
13. Widrow B., Shur D., and Shaffer S. (1981) "On Adaptive Inverse Control." Proceedings of the 15th ASILOMAR Conference on Circuits, Systems, and Computers, 185-195.
14. Burgess J.C. (1981) "Active Adaptive Sound Control In A Duct: A Computer Simulation." Journal of the Acoustical Society of America. Vol 70, 715-726.

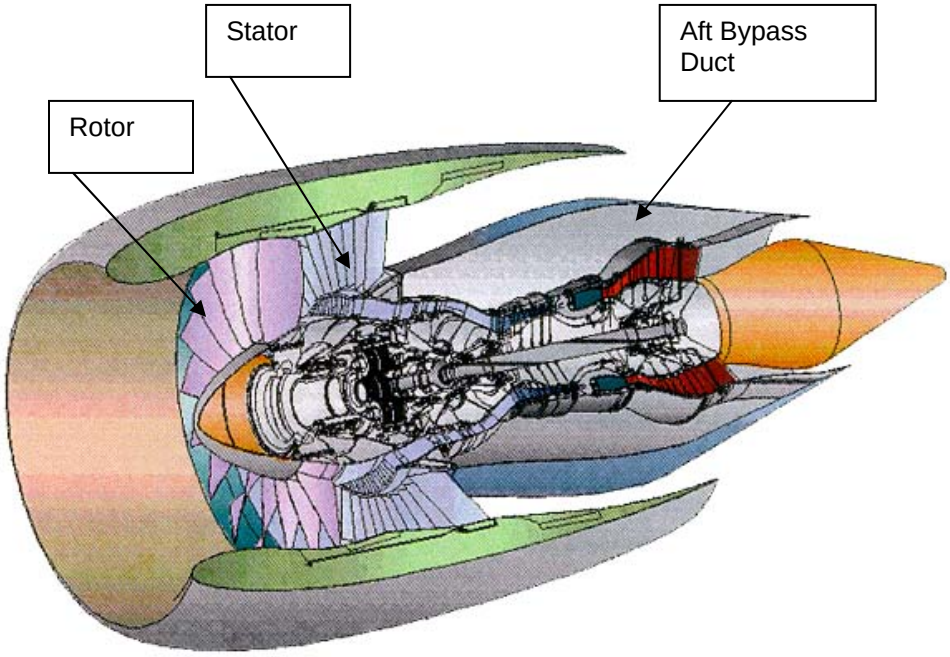

Figure 1. Cut away of high bypass ratio aircraft engine, illustrating fan bypass air duct

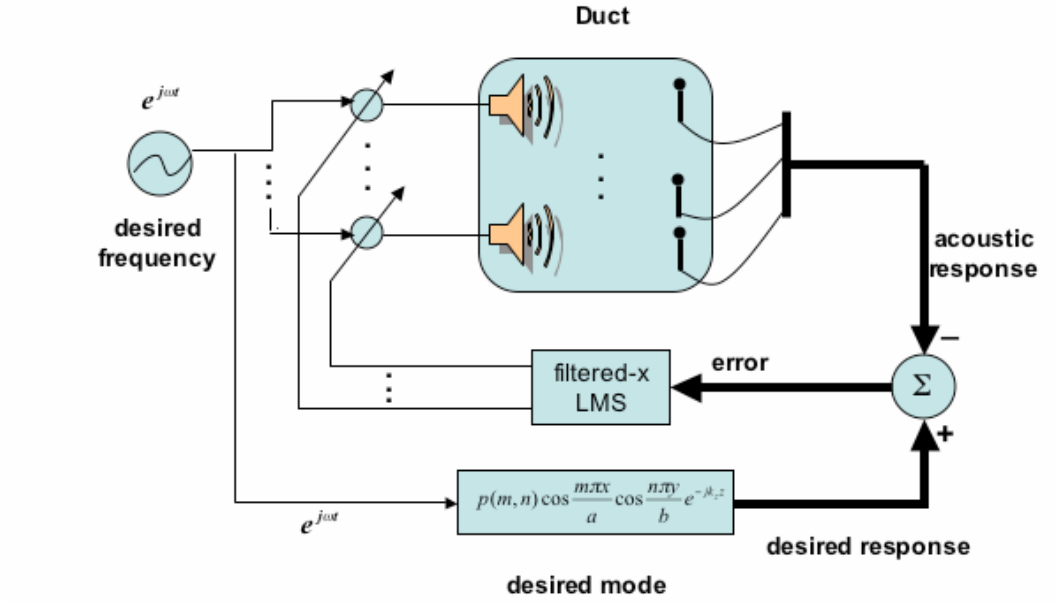

Figure 2. Block Diagram of Control System

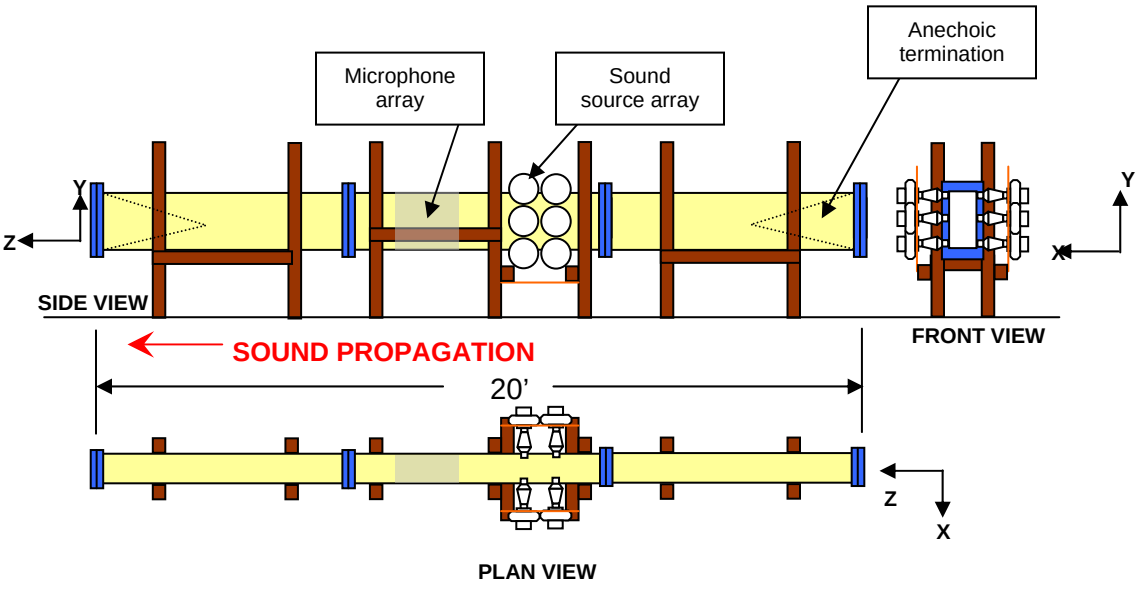

NOTE: Figure not drawn to scale

Figure 3. Prototype Duct for Control System Development

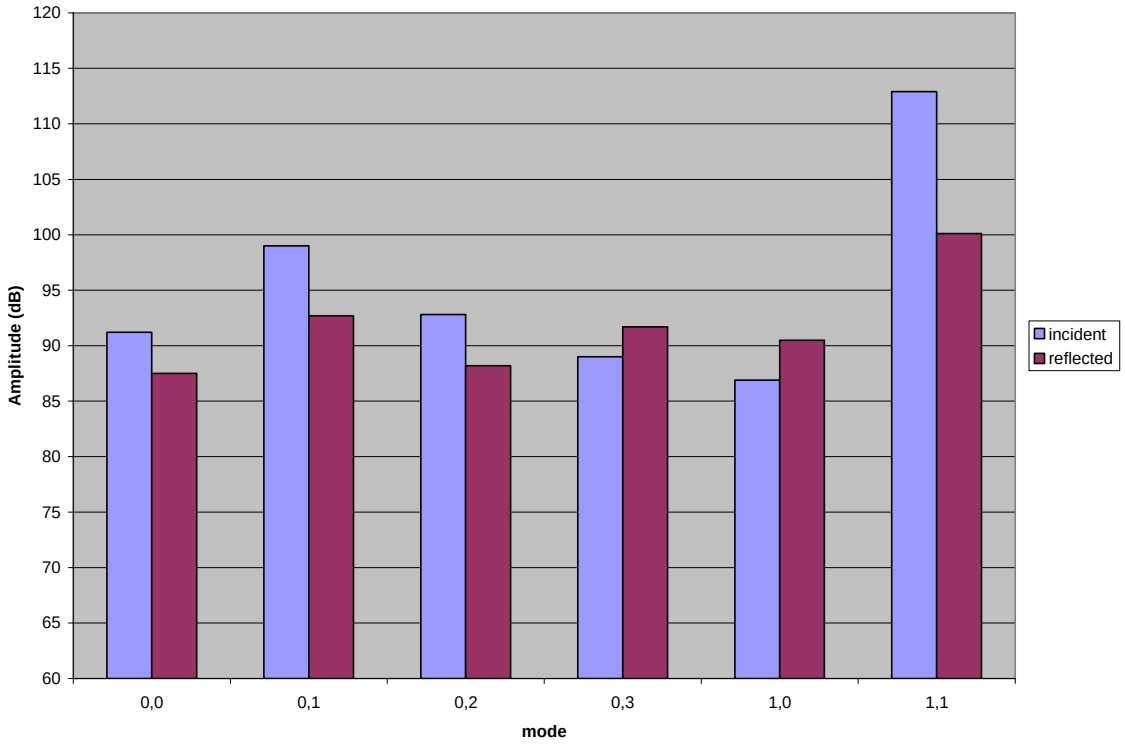

Figure 4. Distribution of modes in rectangular duct, (1,1) mode selected at 970 Hz excitation

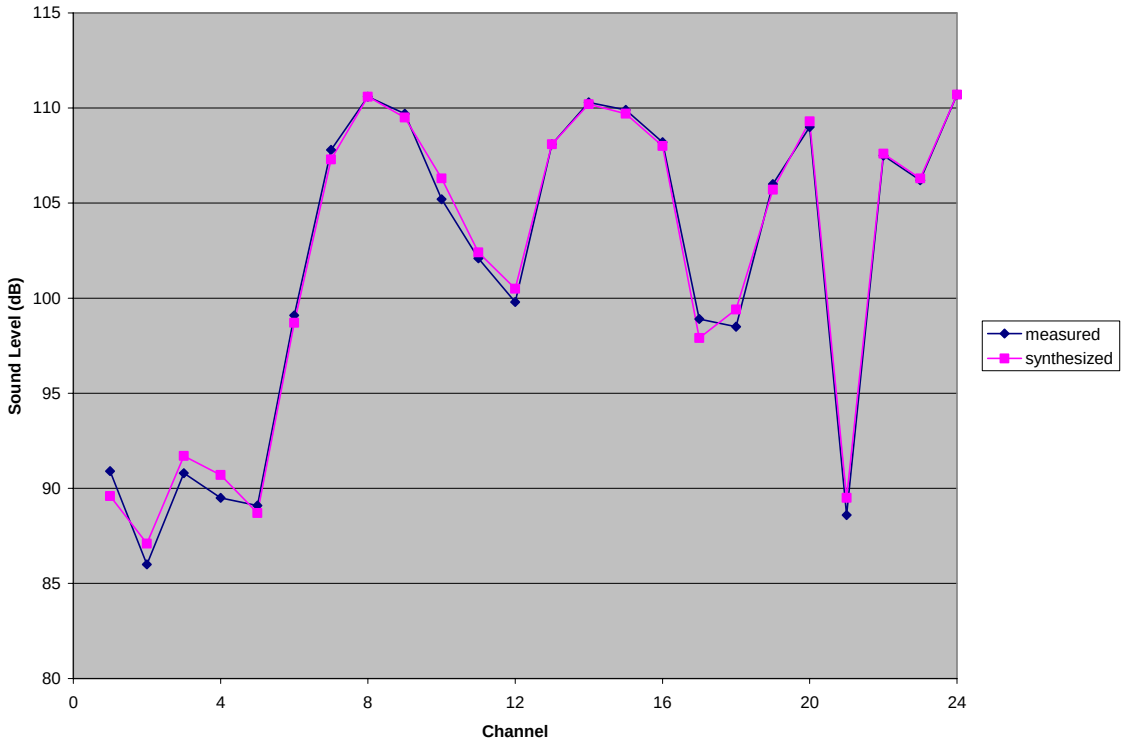

Figure 5. Comparison of measured to synthesized sound pressure level at the sidewall microphone array, for (1,1) selected mode at 1150 Hz.

Table I. Frequencies at which indicated modes cut on in the experiment duct

Mode	0	1	2
0	0	736	1473
1	322	804	1508
2	644	978	1608
3	966	1215	
4	1289	1484	

Table II. Location of Sidewall-Mounted Microphones

Channel	**X (in)**	**Y (in)**	**Z (in)**
1	0.00	10.00	0.00
2	0.00	10.00	2.00
3	0.00	10.00	4.00
4	0.00	10.00	6.00
5	0.00	10.00	8.00
6	0.00	8.75	6.00
7	0.00	5.25	7.00
8	0.00	1.75	8.00
9	0.00	19.25	4.50
10	0.00	15.75	5.50
11	0.00	12.25	1.50
12	0.00	8.75	0.50
13	0.00	5.25	0.25
14	0.00	1.75	1.25
15	0.00	19.25	5.50
16	0.00	15.75	6.50
17	0.00	12.25	6.25
18	0.00	8.75	7.25
19	0.00	5.25	6.00
20	0.00	1.75	7.00
21	4.50	21.00	2.50
22	2.25	21.00	3.50
23	6.50	21.00	2.25
24	1.13	21.00	3.25

Table III. Summary of frequencies and generated modes for evaluation of control system excitation frequency removed from any cut on

Frequency (Hz)	Selected mode 1	Mode Amplitude Ratio	Selected mode 2	Mode Amplitude Ratio	Selected mode 3	Mode Amplitude Ratio
350	(0,1)	+13.7				
500	(0,1)	+24.1				
700	(0,1)	+19.5	(0,2)	+10.4		
770	(0,2)	+13.3	(1,0)	+20.3		
900	(0,2)	+14.4	(1,0)	+8.9	(1,1)	+8.5
1150	(1,1)	+14.6	(0,3)	+10.6	(1,2)	+8.9
1260	(0,3)	-9.6	(1,2)	+1.5	(1,3)	+5.2
1350	(1,2)	+7.9	(1,3)	+2.4	(0,4)	0.0
1550	(0,4)	-10.6	(1,4)	-3.6	(2,1)	-10.1

Table IV. Summary of frequencies and generated modes for evaluation of control system excitation frequency near indicated cut on

Frequency (Hz)	Mode nearest cut on	Cut on ratio	Selected mode 1	Mode Amplitude Ratio	Selected mode 2	Mode Amplitude Ratio
650	(0,2)	1.009	(0,1)	+18.4	(0,2)	+6.8
740	(1,0)	1.005	(0,2)	+8.0	(1,0)	+11.2 (R)
810	(1,1)	1.007	(1,0)	-3.3	(1,1)	+6.7
970	(0,3)	1.004	(1,1)	+12.8	(0,3)	+2.7
985	(1,2)	1.007	(0,3)	+8.8	(1,2)	+7.3 (R)
1220	(1,3)	1.004	(1,2)	-11.2	(1,3)	+7.9 (R)
1295	(0,4)	1.005	(1,3)	+8.5	(0,4)	-14.6
1480	(2,0)	1.005	(0,4)	-3.1	(2,0)	-2.9
1490	(1,4)	1.004	(2,0)	-2.5	(1,4)	+4.3
1610	(2,2)	1.006	(2,1)	-6.1	(2,2)	NC

Table V. Summary of cases for which the controller converged on the incorrect mode

Frequency	Generated Mode	Discussion of failure
810	1,0	Near cut on of 1,1
1220	1,2	Near cut on of 1,3
1260	0,3	Interference with 1,3
1295	0,4	Too few drivers
1350	0,4	Too few drivers
1480	0,4	Too few drivers
1480	2,0	Too few drivers
1490	2,0	Too few drivers
1550	0,4	Too few drivers
1550	1,4	Too few drivers
1550	2,1	Too few drivers
1610	2,1	Too few drivers